End-Linked Poly(dimethylsiloxane) Elastomer Structure: ^{2}H-NMR Transverse Dephasing Data Compared to Predictions of Statistical and Thermodynamic Models

Kimberly McLoughlin, Carol Szeto, T. M. Duncan, and Claude Cohen*

Olin Hall, School of Chemical Engineering, Cornell University, Ithaca, New York 14853-5201

Received January 10, 1996; Revised Manuscript Received April 22, 1996[⊗]

ABSTRACT: ^{2}H-NMR measurements of deuterated poly(dimethylsiloxane) [PDMS(d)] elastomers with systematically varied elastic and swelling properties are presented. ^{2}H-NMR transverse dephasing data are compared to the predictions of a model describing elastomer deuterium transverse dephasing data as a linear superposition of contributions from elastic and pendant chains. Structural parameters obtained from the model for ^{2}H-NMR transverse dephasing are compared to structural parameters inferred from swelling measurements using statistical and thermodynamic models. As predicted by the model for transverse dephasing data, dephasing time constants for elastic chains are directly proportional to number-average molecular weights of elastic chains obtained from swelling measurements.

I. Introduction and Background

Standard techniques for obtaining information about elastomer structure infer molecular-level structure from bulk properties, such as mechanical moduli or polymer concentrations at equilibrium swelling. A more refined understanding of elastomer structure requires the use of experimental techniques which directly probe molecular-level elastomer properties. ^{2}H-NMR has emerged as a powerful tool for such investigations because it is sensitive to elastomer segment orientations and dynamics, through the deuterium quadrupolar interaction.[1−3] The quadrupolar interaction involves the asymmetric nuclear charge distribution, known as a quadrupole moment, which is associated with each deuterium nucleus. A quadrupolar moment experiences a torque in the presence of a local electric field gradient (EFG), which is determined by local molecular structure. The interaction between the quadrupolar moment and the EFG induces an energy splitting whose magnitude depends on the orientation of the EFG. If the EFG is axially symmetric, the magnitude of the deuterium quadrupolar interaction is given (in frequency units) by

$$\omega_Q = \frac{3}{4}\left(\frac{e^2qQ}{\hbar}\right)(3\cos^2\theta - 1) \qquad (1)$$

where $e^2qQ/\hbar$ is the quadrupolar coupling constant and θ is the angle between the EFG and the external magnetic field, B_0.

Typically, deuterium nuclei in isotopically-enriched polymer samples are covalently bonded to carbon atoms. The quadrupolar moment associated with each of these deuterons interacts with the EFG which is approximately axially symmetric and oriented along the C−D bond axis. Thus, ^{2}H-NMR measurement of the distribution of quadrupolar energy splittings experienced by a population of deuterium nuclei directly probes the orientation distribution of C−D bonds in a sample.

The orientation distribution of C−D bonds in a deuterated elastomer is controlled by the orientation distribution of polymer backbone segments. For polymers at temperatures below their glass transition temperatures, these segments are randomly oriented and are fixed in space on the time scale of NMR observation (on the order of 10^{-7} s.) The quadrupolar frequency distribution corresponding to an isotropic distribution of fixed C−D bonds gives a broad spectrum known as a Pake pattern,[4] which is characteristic of rigid solids. In polymer samples, if the C−D bonds belong to a side group such as a methyl group, the Pake pattern is narrower (by a factor of 3 in the case of methyl groups) than for a rigid solid due to side group rotation even below the glass transition. The ^{2}H-NMR spectrum of deuterated poly(dimethylsiloxane) [PDMS(d)] below its glass transition temperature (T_g(PDMS) = 153 K) shown in Figure 1a provides an example of this characteristic spectrum.

Above the glass transition temperature, each C−D bond orientation becomes time-dependent due to segment motion. The averaging of the quadrupolar interaction due to segment motion is described by the following expression, in which the bar represents a time average:

$$\bar{\omega}_Q = \frac{3}{4}\left(\frac{e^2qQ}{\hbar}\right)\overline{[3\cos^2\theta(t) - 1]} \qquad (2)$$

Thus, motion averages the quadrupolar interaction and narrows the ^{2}H-NMR spectrum. In the limit of rapid, isotropic segment motion, the quadrupolar interaction is completely averaged, and the ^{2}H-NMR spectrum is reduced to a sharp peak at the central frequency. This limit is approached by segment motions with correlation time, τ_C, at least an order of magnitude shorter than the duration of the NMR experiment, which is determined by the inverse width of the quadrupolar frequency distribution, ω_Q^{-1} ($\sim 10^{-6}$ s). An unentangled PDMS(d) melt at room temperature satisfies the assumptions of this extreme narrowing condition and gives a ^{2}H-NMR spectrum devoid of quadrupolar character, as shown in Figure 1c.

^{2}H-NMR spectra have been reported for a variety of elastomers above their glass transition temperatures.[5−8] The spectrum of a typical PDMS(d) elastomer given in Figure 1b demonstrates that ^{2}H-NMR spectra of elastomers lack the singularities and breadth of the Pake pattern characteristic of rigid isotropic solids. However, they are significantly broader than spectra correspond-

[⊗] Abstract published in *Advance ACS Abstracts,* July 1, 1996.

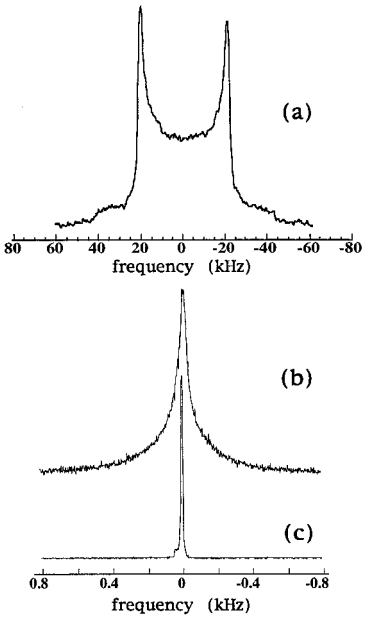

Figure 1. ^{2}H-NMR spectra of deuterated poly(dimethylsiloxane) [PDMS(d)]: (a) un-cross-linked precursor chains at 153 K; (b) elastomer at 298 K; (c) un-cross-linked precursor at 298 K. Note that the lower scale is expanded by a factor of 100 relative to the upper scale.

ing to un-cross-linked polymer melts. Thus, elastomer ^{2}H-NMR spectra represent residual, motion-averaged quadrupolar frequency distributions corresponding to rapid, *nonisotropic* segment motion. Interpretation of ^{2}H-NMR data in terms of elastomer structure and dynamics requires a quantitative description of residual quadrupolar frequency distributions in terms of physical parameters.

Recently, a model has emerged which describes the residual deuterium quadrupolar frequency distribution observed by ^{2}H-NMR of elastomers as a linear superposition of two distinct components.[9,10] One component is attributed to elastic chains, which are attached to the elastomer network at both ends, and the other is attributed to pendant chains, which are bound to the network at only one end. According to this model, the pendant chain contribution to the residual quadrupolar frequency distribution is expected to experience more motional averaging than does the elastic chain component, due to mobility differences between the two types of chains. Hence, this model predicts that the portion of the ^{2}H-NMR spectrum corresponding to pendant chains is significantly narrower than the portion corresponding to the elastic chains. This two-component model has been tested qualitatively using ^{2}H-NMR observations of highly-entangled polystyrene chains composed of deuterated and nondeuterated blocks.[9] The spectra of labeled blocks near chain ends, which were used to model pendant chains, were significantly narrower than spectra of blocks near chain centers, which were used to represent elastic chains.

Other investigators have obtained ^{2}H-NMR data for randomly-cross-linked *cis*-polybutadiene elastomers to quantitatively test the two-component representation of ^{2}H-NMR observations of elastomers.[10] After a component attributed to soluble material was subtracted, the data were well represented by a sum of two distinct contributions, one attributed to elastic chains, and the other to pendant chains. For elastic chain molecular weights (M_c) ranging from approximately 5.5 to 8.8 kg/mol, as estimated from mechanical measurements, the NMR transverse dephasing rate for deuterons in elastic chains was correlated to M_c. The authors concluded that ^{2}H-NMR may be used to determine average molecular weights between cross-links of elastic networks. Their investigation also suggested that the ^{2}H-NMR data could be interpreted to determine additional elastomer structural parameters, including the weight fractions of elastic and pendant chains.

To further assess the sensitivity of ^{2}H-NMR to elastomer structure and to examine the two-component model for elastomer ^{2}H-NMR data, we have obtained ^{2}H-NMR data for deuterated PDMS elastomers with systematically varied elastic properties. The end-linking procedure used herein has several advantages over random cross-linking and other network-formation techniques. One advantage is that it produces networks with low amounts of soluble material, which can be eliminated by careful swelling procedures prior to NMR observations. Additionally, this end-linking procedure leads to the formation of well-defined networks whose mechanical and swelling properties have been studied extensively.[11,12] We have produced end-linked networks with molecular weights between effective cross-links which vary from below 10 kg/mol to above 70 kg/mol, and we have determined their structural parameters independent of NMR results. Specifically, average molecular weights and weight fractions of elastic chains of these networks have been determined, based on mechanical and swelling properties. Finally, the end-linking technique used in this study has the advantage that it can be used to obtain selectively-deuterated networks; we report ^{2}H-NMR observations of randomly-deuterated networks and of networks in which only portions of pendant material are deuterated.

II. Experimental Section

Elastomer Synthesis. Poly(dimethylsiloxane) (PDMS) elastomers were produced by end-linking polymer precursors with a tetrafunctional cross-linking agent (A_4) using a technique refined by Patel et al.[11] to produce networks with controlled and varied properties. Vinyl-terminated PDMS precursors were end-linked via platinum-catalyzed hydrosilation using tetrakis(dimethylsiloxy)silane (obtained from Hüls) as a cross-linking agent. Neat difunctional (B_2) and monofunctional (B_1) polymer precursors were combined in carefully-controlled ratios with the cross-linking agent (A_4). A platinum catalyst, *cis*-dichlorobis(diethyl sulfide)platinum-(II) (from Strem Chemical Co.) was dissolved in a minimal amount of toluene and added to the reaction mixture to achieve a concentration of 20 parts Pt per 10^6 parts siloxane. Networks were cured in polyethylene molds at 35 °C under vacuum; the low curing temperature has been demonstrated to minimize side reactions.[13]

B_2 and B_1 were produced by polymerizing hexamethylcyclotrisiloxane (D_3), using insertion polymerization techniques developed to minimize polydispersity and branching.[14−16] B_2 was produced by polymerizing D_3 in toluene, using water as an initiator, dimethyl sulfoxide (DMSO) as a promoter, and benzyltrimethylammonium bis(*o*-phenylenedioxy)phenylsiliconate as a catalyst. B_1 was produced by polymerizing D_3 in cyclohexane, using *n*-BuLi as an initiator and DMSO as a promoter. Both types of precursors were end-capped with vinyl groups using vinyldimethylchlorosilane (from Hüls). Nondeuterated D_3 was obtained from Hüls Chemical Co.; perdeuterated D_3 was synthesized using methods described below. Polymer precursors were characterized using gel permeation chromatography (GPC) with toluene as the carrier solvent. Molecular weights and polydispersities were calculated from GPC data; Mark−Houwink parameters obtained by Lapp et al.[17] were used to convert polystyrene-equivalent molecular weights to PDMS molecular weights.

Table 1. End-Linking Reactant Concentrations and Network Parameters from Extraction and Swelling Experiments

sample	r^a	x^b	W_{sol}	v_2
Deuterated Networks $M_{n,B_2} = 19$ kg/mol; $M_{n,B_1} = 16$ kg/mol				
A-1	1.7	0.000	0.0061	0.279
A-2	1.6	0.099	0.0232	0.262
A-3	1.6	0.173	0.0480	0.242
A-4	1.1	0.000	0.1410	0.147
A-5	1.2	0.301	0.3010	0.105
Protonated Networks with Deuterated Monofunctional Chains $M_{n,B_2} = 16$ kg/mol; $M_{n,B_1} = 16$ kg/mol				
B-1	1.7	0.026	0.0122	0.280
B-2	1.7	0.081	0.0292	0.268
B-3	1.7	0.217	0.0961	0.182
Protonated Networks $M_{n,B_2} = 26$ kg/mol; $M_{n,B_1} = 29$ kg/mol				
C-1	1.7	0.000	0.0118	0.254
C-2	1.7	0.307	0.0888	0.175
C-3	1.7	0.569	0.2290	0.102

^{a} $r = 4A_4/(B_1 + 2B_2)$. ^{b} $x = B_1/(B_1 + B_2)$.

To produce precursors containing randomly-distributed perdeuterated dimethylsiloxane units, mixtures of 30 wt % perdeuterated D_3 and 70% nondeuterated D_3 were polymerized. Both deuterated and nondeuterated D_3 monomers used to produce the partially-deuterated precursors were synthesized using a reaction sequence adapted from the method described by Beltzung et al.,[18] which produces a mixture of cyclic siloxane trimers (D_3) and tetramers, octamethylcyclotetrasiloxane (D_4). The weight percent of perdeuterated siloxane units incorporated into each of the partially-deuterated precursors was determined by ^{2}H-NMR.

Three types of PDMS networks were prepared. The first series of networks, labeled A-1 through A-5, was produced by end-linking deuterated B_2 and deuterated B_1. The second series of networks, labeled B-1 through B-3, was produced by end-linking nondeuterated B_2 and deuterated B_1. The third series of networks, labeled C-1 through C-3, was produced by end-linking nondeuterated B_2 and nondeuterated B_1. Networks in the A, B, and C series were cured in molds and then used in swelling and in ^{2}H-NMR experiments. Two additional networks were produced by end-linking nondeuterated B_2 and nondeuterated B_1. These networks were cured between the plates of a Rheometrics RDA II rheometer at room temperature for at least 36 h. They were used in dynamic mechanical and swelling measurements to confirm the correlation between polymer volume fraction at swelling equilibrium and dry network storage modulus reported by Patel et al.[11]

Experimental characteristics for PDMS networks are given in Table 1. Relative amounts of B_2 and B_1 added to the end-linking mixture are reported as x, the mole fraction of monofunctional chains:

$$x = B_1/(B_1 + B_2) \tag{3}$$

where B_1 and B_2 are moles of monofunctional and difunctional precursor chains, respectively. The ratio of silane sites on tetrafunctional cross-link molecules to vinyl end groups on precursor chains is reported as r,

$$r = 4A_4/(B_1 + 2B_2) \tag{4}$$

where A_4 is the number of moles of cross-linking agent used in the end-linking reaction mixture. Networks produced using $x = 0$ and r approximately equal to 1.7 have been found previously to contain minimum amounts of soluble material and to exhibit minimum volume fractions of polymer at equilibrium swelling; they have been referred to as "model" networks.[11]

Nondeuterated PDMS networks containing deuterated PDMS(d) probe chains were produced by placing small amounts (<10 wt %) of probe chains upon the surfaces of the PDMS networks labeled C-1 through C-3. The networks were then covered with overturned glass vials and placed in an oven at 60 °C. Chains were assumed to be dissolved and uniformly distributed throughout the networks when network surfaces appeared to be completely dry (after approximately 3 days.)

Elastomer Characterization. Elastomer networks were characterized using swelling and extraction measurements, dynamic mechanical analysis, and ^{2}H-NMR. Swelling and extraction were performed in toluene using standard techniques.[19] Soluble fractions, W_{sol}, were determined by weighing networks before and after toluene extraction of solubles. Equilibrium polymer volume fractions, v_2, were calculated by assuming no volume change upon mixing, using the following expression:

$$v_2 = 1 + \left(\frac{m_s - m_{ex}}{m_s}\right)\left(\frac{\rho_2}{\rho_1}\right) \tag{5}$$

in which m_s represents the mass of network plus solvent at equilibrium swelling, m_{ex} represents the mass of a dry network after extraction of soluble material, and ρ_2 and ρ_1 are the room temperature (25 °C) densities of polymer and solvent, respectively. Weight fractions of soluble material extracted from the networks, W_{sol}, and weight fractions of polymer at swelling equilibrium, v_2, are given in Table 1.

Mechanical measurements were obtained using the parallel-plate geometry of the rheometer. The plates were 25 mm in diameter, and the gap between the plates was 0.8 mm. Storage and loss moduli of networks cured between the rheometer plates were measured in oscillatory shear in air at room temperature.

^{2}H-NMR data was obtained on a Bruker CXP200 spectrometer operating at 30.72 MHz. Spectra were obtained by Fourier transforming the decay stimulated by a standard $(90°)_x$ pulse, with duration typically 5 μs. Transverse dephasing data were obtained using a $(90°)_x-\tau-(180°)_y-\tau$ pulse sequence, in which delay times, τ, were varied between 0.1 and 9 ms.

III. Results

Number-average molecular weights of polymer precursors obtained using GPC are indicated in Table 1 above the characteristics of the networks into which they were incorporated; polydispersities of precursors were found to be less than or equal to 1.1. ^{2}H-NMR spin-counting measurements indicated that 24 wt % of the dimethylsiloxane units in the B_2 chains were perdeuterated; 25 wt % of the siloxane units in the B_1 chains were perdeuterated. Network characteristics obtained from extraction and swelling experiments (given in Table 1) demonstrate that the amount of soluble material, W_{sol}, and the polymer volume fraction at equilibrium swelling in toluene, v_2, depend on end-linking reactant concentrations given by r and x.

^{2}H-NMR spectra obtained using $(90°)_x$ pulse experiments are reported in Figure 2 for PDMS(d) networks in series A, produced by end-linking deuterated monofunctional and deuterated difunctional precursors. Intensity at each frequency, $I(\omega_i)$, is proportional to the fraction of deuterium nuclei which experience an average, local magnetic field which has magnitude ω_i (in frequency units). Although the local fields experienced by deuterium nuclei are dominated by the large deuterium quadrupolar interaction, they are also influenced by other local magnetic interactions and by inevitable spatial inhomogeneities in the external magnetic field, B_0.

More precise observations of residual quadrupolar frequency distributions have been obtained using experiments that isolate the influence of the quadrupolar interaction on local magnetic fields, eliminating contributions from magnetic field inhomogeneities and other

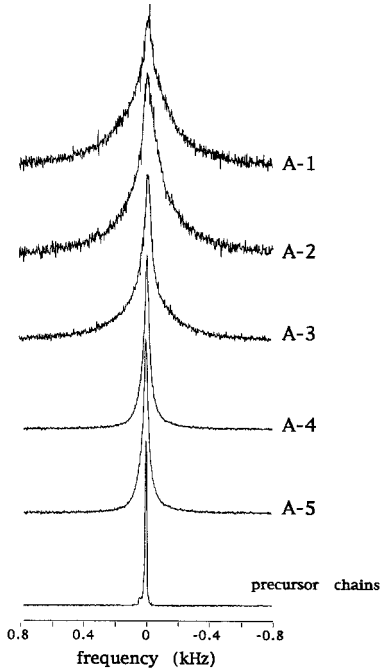

Figure 2. ^{2}H-NMR spectra of PDMS(d) networks produced by end-linking partially-deuterated difunctional precursor chains with varying amounts of partially-deuterated monofunctional precursor chains. (See Table 1).

static magnetic interactions. These experiments report quadrupolar frequency distributions in terms of their influence on the time evolution of magnetization, $M(t)$, in the plane perpendicular to B_0. Following a $(90°)_x$ pulse, which rotates magnetization into the plane perpendicular to B_0, transverse magnetization dephases due to the distribution of local magnetic interaction frequencies. Transverse magnetization may be expressed as a sum of cosine functions:

$$\frac{M(t)}{M_0} = \sum_i \cos(\omega_i t) \tag{6}$$

where M_0 gives the magnetization observed immediately after the rotation of spins into the transverse plane. The sum in eq 6 is over all ^{2}H spins. This dephasing of transverse magnetization is observed using a $(90°)_x-\tau-(180°)_y-\tau$ pulse sequence, which isolates the dephasing of transverse magnetization induced by the quadrupolar interaction during time $t = 2\tau$. Using a series of $(90°)_x-\tau-(180°)_y-\tau$ pulse sequences and measuring the intensity of magnetization observed for various τ delays, the dephasing of the transverse magnetization due to fluctuations in the averaged local quadrupolar interaction is monitored as a function of time. The ^{2}H-NMR transverse dephasing data obtained by this technique for deuterons in PDMS(d) networks in series A are given in Figure 3. ^{2}H-NMR transverse dephasing data for deuterons in PDMS(d) networks in series B are given in Figure 4b, and dephasing data for deuterons in PDMS(d) probe chains dissolved in the protonated networks of series C are given in Figure 4a.

IV. Discussion

Network Structure Inferred from Macroscopic Properties. We determined structural parameters of PDMS networks from macroscopic properties using the statistical model of nonlinear polymerization developed by Macosko and Miller.[20−22] Application of the model

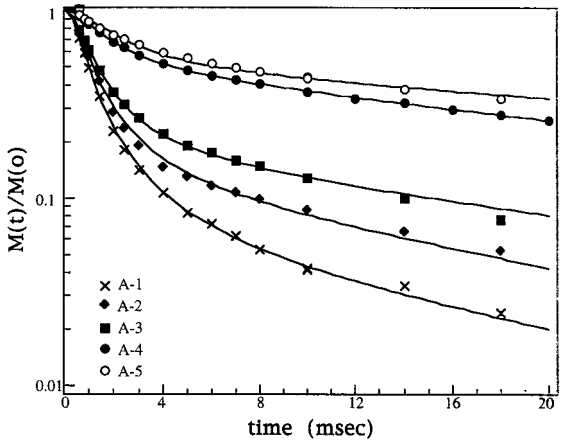

Figure 3. ^{2}H-NMR transverse relaxation functions for PDMS-(d) networks produced by end-linking partially-deuterated difunctional precursor chains with varying amounts of partially-deuterated monofunctional precursor chains. Solid curves are best fits using eq 24.

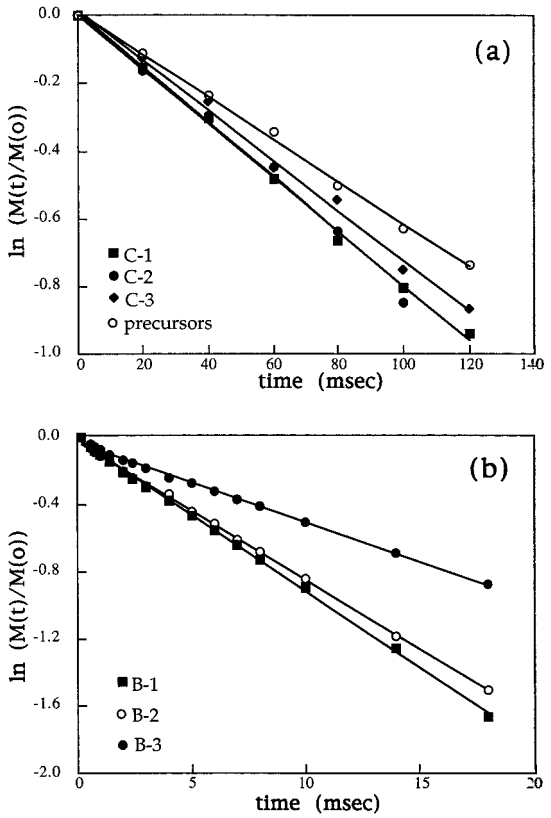

Figure 4. ^{2}H-NMR transverse relaxation of (a) PDMS(d) probe chains dissolved in nondeuterated PDMS networks and (b) PDMS networks produced by end-linking nondeuterated difunctional precursors with varying amounts of partially-deuterated monofunctional chains. Solid lines represent best fits to eq 18.

gives an expression for the weight fraction of soluble material, W_{sol}, in a newly-formed network in terms of weight fractions, W_i, of each species, i, used in the reaction mixture.

$$W_{sol} = W_{A_4}\alpha^4 + W_{B_2}\beta^2 + W_{B_1}\beta \tag{7}$$

α and β represent probabilities of events defined in the formalism developed by Macosko and Miller. Calculation of α and β using the model gives an expression for W_{sol} in terms of reaction mixture concentrations and p, the extent of reaction of silane groups (A) with vinyl

Table 2. Network Parameters from Statistical and Thermodynamic Models

sample	f_{el}	$M_{n,el}$ (kg/mol)	M_c (kg/mol)
Deuterated Networks			
A-1	0.86	30	9.6
A-2	0.73	32	11
A-3	0.62	37	13
A-4	0.46	39	38
A-5	<0.29	>58	71
Protonated Networks with Deuterated B_1			
B-1	0.80	26	9.5
B-2	0.70	30	11
B-3	0.50	37	25
Protonated Networks			
C-1	0.80	42	12
C-2	0.48	57	27
C-3	0.24	86	75

end-groups (B). Using experimental values for reaction mixture concentrations, the equation may be solved iteratively to identify a value for p which yields a value for W_{sol} that agrees with the experimental value. Once p is thus obtained, numerical values for α and β are used to determine the weight fraction of elastic chains, f_{el}, in the network:

$$f_{el} = \frac{W_{el}}{W_{el} + W_{pen}} \tag{8}$$

Further application of the model gives an expression for the number-average molecular weight of elastic chains:

$$M_{n,el} = 2M_A + \frac{M_{n,B_2} + (M_{A_4} - 2M_A)C}{1 - C} \tag{9}$$

where M_{A_4} is the molecular weight of a tetrafunctional cross-link molecule, M_A is the molecular weight of one arm of a cross-link junction, and C is

$$C = \frac{3\alpha^2(1-\alpha)}{3\alpha^2(1-\alpha) + 3\alpha(1-\alpha)^2 + 3(1-\alpha)^3} \tag{10}$$

Values of f_{el} and $M_{n,el}$ calculated using these expressions for our networks are presented in Table 2.

An alternate approach for obtaining structural parameters from macroscopic measurements uses the Flory−Rehner model,[23] which describes the equilibrium swelling behavior of elastic networks. At swelling equilibrium, this model leads to expressions for structural parameters in terms of v_2, the polymer volume fraction at equilibrium swelling, and χ, the polymer/solvent interaction parameter. Use of the affine model[24] for the elastic properties of the networks gives ν, the number of moles of elastic chains per unit volume in the network, in terms of v_2 and the molar volume of the solvent, V_1:

$$\nu = \frac{\ln(1 - v_2) + v_2 + \chi v_2^{\,2}}{V_1\left(\frac{v_2}{2} - v_2^{\,1/3}\right)} \tag{11}$$

Use of the phantom model[25] gives an expression for the cycle rank, $(\nu - \mu)$ of the network:

$$\nu - \mu = \frac{\ln(1 - v_2) + v_2 + \chi v_2^{\,2}}{-V_1 v_2^{\,1/3}} \tag{12}$$

where μ is the number of moles of junctions per unit volume. The polymer/solvent interaction parameter, χ, for PDMS networks swollen in toluene is estimated using an expression developed for PDMS chains dissolved in toluene:

$$\chi = 0.445 + 0.297 v_2 \tag{13}$$

The applicability of this expression to PDMS networks swollen in toluene has been verified experimentally by Patel et al.[11] The molar volume of toluene is taken to be 106.9 cm^3/mol.

Storage moduli may be calculated from structural parameters obtained from swelling measurements, using an expression based on the affine model:

$$G_e/RT = \nu \tag{14}$$

or using an expression based on the phantom model:

$$G_e/RT = \nu - \mu \tag{15}$$

Because $v_2/2$ is much smaller than $(v_2)^{1/3}$ for most of the networks used in this study, the storage moduli evaluated using (11) and (14) do not differ appreciably from those obtained using (12) and (15). An alternative to calculating storage modulus, G_e, based on swelling data is to obtain experimental values of storage modulus using dynamic mechanical analysis on dry networks. An estimate for the number-average molecular weight, M_c, between effective cross-links may be obtained from the storage modulus by assuming the affine model for elasticity. Based on this model, the molecular weight between effective cross-links is taken to be

$$M_c = \frac{\rho}{G_e/RT} \tag{16}$$

We have obtained values for M_c from swelling results by combining expressions 12, 15, and 16; these values are reported in Table 2. Equation 16 has also been used to calculate number-average molecular weights between effective cross-links from storage moduli obtained from mechanical results. These values were in excellent agreement with those obtained from swelling results, confirming the correlation between v_2 and storage modulus reported by Patel et al.[11]

The correlation between the structural parameters which are reported in Table 2 and the end-linking mixture concentrations reported in Table 1 demonstrates that network structure as obtained from the models presented above is controlled by, and varies with, the mole fraction of monofunctional chains, x, and the ratio of cross-link sites to vinyl end groups, r. Specifically, end-linking B_2 with systematically increasing amounts of B_1 produces networks with decreasing fractions of elastic chains (f_{el}) and increasing number-average molecular weights of elastic chains ($M_{n,el}$). A comparison of structural properties of networks A-1 and A-4 suggests that the same results could be obtained by simply varying r. These observations are in good agreement with results reported by Patel et al.,[11] which show that networks with maximum f_{el} are produced when r values are held at approximately $r^{opt} = 1.7$ and x is zero.

The observed decrease in f_{el} with increasing amounts of monofunctional precursor is expected because a given monofunctional chain can attach to the elastic network at only one site. Thus, each monofunctional chain attached to the elastic network contributes to the weight

fraction of pendant material. The increase in number-average molecular weight of elastic chains predicted by the statistical model with decreasing fractions of elastic chains may be explained in terms of a decrease in the density of cross-link junctions. In the statistical model, a cross-link is defined as a chemical junction from which at least three paths loop back to the network. A tetrafunctional cross-link molecule to which two or more pendant chains are attached does not meet this definition of a cross-link. An elastic chain is defined as the polymer backbone material which extends between two cross-links. Thus, the density of cross-links decreases, and the average molecular weight of elastic chains increases as the fraction of elastic chains decreases. Similarly, we expect pendant chain molecular weights to increase as f_{el} decreases.

As f_{el} decreases, both the number-average molecular weight of elastic chains, $M_{n,el}$, obtained using the statistical model and the molecular weight between effective cross-links, M_c, obtained from swelling results increase. However, the number-average molecular weights of elastic chains obtained using the statistical model are consistently larger than those obtained from the swelling model, as shown in Table 2. The discrepancy between the two models increases systematically as the fraction of elastic chains increases. The difference between the models may be explained by examining the definitions of elastic chains inherent in each model. The statistical model defines an elastic chain as the material extending between two chemical cross-links, which have been strictly defined as covalent chemical junctions from which at least three paths loop back to the network. In contrast, the swelling model has no such criteria for cross-links. The presence of effective cross-links, which may include topological interactions as well as chemical junctions, is inferred from elastic resistance to swelling. Thus, the molecular weights of elastic chains obtained from the swelling model correspond to polymer backbone material extending between any constraints which act as effective cross-links, including both chemical cross-link junctions and trapped topological entanglements. Because the number of entanglements plus cross-links is always greater than the number of cross-links alone, the density of effective cross-links obtained from the swelling model exceeds that obtained from the statistical model. Thus, the molecular weight of material extending between constraints obtained from the statistical model is consistently larger than that obtained from the swelling model. The discrepancy decreases as the fraction of elastic chains decreases because loose networks with large fractions of pendant chains do not trap entanglements effectively. For networks with low f_{el}, the density of effective constraints is essentially equal to the density of chemical cross-link junctions, and the average molecular weight of elastic chains obtained from the statistical model approaches that obtained from swelling results.

Network Structure Inferred from ^{2}H-NMR. To investigate the relationship between ^{2}H-NMR observations of elastomers and molecular-level network structure, spectral features of PDMS(d) networks were compared to structural parameters inferred from macroscopic properties. ^{2}H-NMR spectra obtained by observing the PDMS(d) networks produced using deuterated difunctional and deuterated monofunctional precursors are given in Figure 2. The uppermost spectrum corresponds to the network with the greatest fraction of elastic chains (f_{el}) and the lowest number-average molecular weight of elastic chains ($M_{n,el}$). As f_{el} decreases and $M_{n,el}$ increases, network spectra become narrower. However, all network spectra are significantly broader than that of the un-cross-linked precursors. Because the quadrupolar frequency distribution is averaged by motions of the elastomer chain segments, these observations may be explained in terms of segment mobility. In the limit of rapid, isotropic segment motion ($\tau_c \ll \omega_Q^{-1} \ll 10^{-6}$ s), the quadrupolar interaction is completely averaged, and the ^{2}H-NMR spectrum is reduced to a sharp peak at the central frequency. Therefore, the narrow precursor chain spectrum indicates that segment motion in the polymer melt is both rapid and isotropic. In contrast, the broader network spectra indicate that segment motion is anisotropic and/or is not sufficiently rapid on the NMR time scale to completely average the quadrupolar interaction. Specifically, the systematic broadening observed for networks with increasing f_{el} and decreasing $M_{n,el}$ indicates that segment mobility decreases as expected with increasing density of effective cross-links.

Interpretation of ^{2}H-NMR observations in terms of elastomer structure requires the use of theoretical models which describe motion-averaged segment orientation distributions in terms of structural parameters. Such theoretical models rely on the assumption that the motion-averaged quadrupolar interaction dominates ^{2}H-NMR data. Thus, to obtain ^{2}H-NMR data for comparisons with the predictions of theoretical models, an experimental technique is used which isolates the effect of the quadrupolar interaction from distortions caused by field inhomogeneities and other static magnetic interactions, which are typically 30−40 Hz. The technique uses a series of $(90°)_x-\tau-(180°)_y-\tau$ pulse sequences to observe transverse magnetization as a function of time. Transverse magnetization dephases as a function of time due to the distribution of local frequencies experienced by deuterium spins in a given sample. Specifically, the motion-averaged quadrupolar frequency distribution is reflected in the rate and shape of the dephasing data. Transverse dephasing data are given in Figure 3 for PDMS(d) networks in series A, which have been produced from deuterated difunctional and deuterated monofunctional precursors. The broad distribution of quadrupolar frequencies experienced by deuterons in networks with high f_{el} and low $M_{n,el}$ corresponds to the rapid quadrupolar dephasing observed in the lowest curve of Figure 3. As segment motion increases, the residual quadrupolar frequency distribution narrows (Figure 2), and the transverse dephasing rate decreases (Figure 3).

To develop a model for transverse dephasing of elastomer magnetization, several authors have suggested that two distinct motional processes average the segment orientation distribution reflected in the dephasing data.[9,10,26−28] This two-component model was initially proposed to describe dephasing observed for transverse proton magnetization in elastomers. (Transverse proton dephasing is dominated by the homonuclear proton dipolar interaction, which, like the quadrupolar interaction, is determined by local structure. Whereas the quadrupolar interaction is determined by the orientation distribution of C−D bonds, the dipolar interaction is determined by the orientation distribution of ^{1}H−^{1}H internuclear vectors.[1]) The earliest two-component model for elastomer transverse dephasing simply predicted a "slowly" dephasing com-

Table 3. ^{2}H-NMR Parameters for PDMS(d) Precursors

precursor dissolved in	probe concn (wt %)	$t_{precursor}$ (ms)
network C-1	9.34	125
network C-2	8.60	124
network C-3	8.30	135
melt		160

ponent, corresponding to a fast motional process, and a "rapidly" dephasing component, attributed to a slower motional process.[26] More recent models associate the slowly dephasing component with segments in pendant chains, whose motion is relatively less hindered, and the fast dephasing process to segments in elastic chains, whose motion is restricted due to constraints at both ends of the chains.[9,10] Transverse dephasing data expected to result from these two motional processes can be represented as the linear superposition of a contribution from deuterons in elastic chains, $E(t)$, and a contribution from deuterons in pendant chains, $P(t)$:

$$M(t)/M_0 = f_{el}E(t) + (1 - f_{el})P(t) \tag{17}$$

The contributions are weighted by the fractions of elastic and pendant chains, which give the fractions of deuterons in elastic and pendant chain segments, respectively. Analytic expressions for $E(t)$ and $P(t)$ in terms of elastomer structure may be obtained by modeling the distinct motional processes experienced by elastic and pendant chains.

Pendant Chain Contribution. A theoretical description of transverse dephasing resulting from orientation-dependent interactions which are averaged completely on the time scale of NMR observation has been developed by Bloembergen, Purcell, and Pound.[29] Based on their formalism, transverse dephasing of deuterons is well represented by an exponential decay, provided that motion is isotropic and sufficiently rapid ($\tau_c \ll \omega_Q^{-1}$) that the time-averaged quadrupolar interaction is zero. In this limit, the characteristic transverse dephasing time, $t_{transverse}$, increases as the correlation time of segment motion, τ_c, decreases.[30]

Dephasing data for un-cross-linked, un-entangled linear polymer chains above their glass transition temperatures have been found to be well represented by this formalism, as demonstrated in Figure 4a, in which the uppermost transverse dephasing data correspond to PDMS(d) precursor chains (M_n = 16 kg/mol). The solid line represents the best fit of the data to a single exponential with time constant, $t_{precursor}$, given in Table 3. Because dephasing data for the precursor chains are well represented by an exponential decay, it may be inferred that segment motions in the precursor chains average the quadrupolar interaction completely. Similar results are obtained for linear PDMS(d) chains (M_n = 16 kg/mol) dissolved in protonated PDMS networks. Transverse dephasing data for deuterated precursor chains dissolved in protonated networks are also shown in Figure 4a; solid lines represent best fits of the data to single exponentials with time constants, $t_{precursor}$, given in Table 3. Characteristic dephasing times for the dissolved chains are somewhat shorter than for neat precursor chains of the same molecular weight. The shorter dephasing times for dissolved chains indicate that correlation times for segment motions are, on average, longer for precursor chains dissolved in networks than for chains in the melt.

^{2}H-NMR transverse dephasing data for networks produced by end-linking deuterated monofunctional polymer precursors and protonated difunctional precursors are given in Figure 4b. They represent direct ^{2}H-NMR observations of pendant chains in elastic networks, because only pendant chains or portions of pendant chains in these networks were deuterated. Solid lines in Figure 4b represent best fits of pendant chain dephasing data to single exponential decays, $P(t)$, with time constants t_{pen}:

Table 4. Network Parameters from ^{2}H-NMR Measurements

sample	f_{el}	t_{el} (ms)	t_{pen} (ms)
Deuterated Networks			
A-1	0.95	3.7	16
A-2	0.89	4.1	18
A-3	0.84	4.6	29
A-4	0.52	6.7	30
A-5	0.51	8.5	50
Protonated Networks with Deuterated B_1			
B-1			11
B-2			12
B-3			21

$$P(t) = \exp(-t/t_{pen}) \tag{18}$$

Multiple-exponential fits were also tested but did not yield statistically better fits to the data. Thus, we find that transverse deuterium dephasing curves for pendant material are well represented by single-exponential decays. Characteristic times for pendant chain dephasing, t_{pen}, are given in Table 4. They are an order of magnitude shorter than those obtained for unattached chains dissolved in networks, indicating that the cross-links which attach pendant chains to elastic networks decrease the average correlation time, τ_c, for pendant chain segmental motions.

Elastic Chain Contribution. Cohen-Addad[31] has demonstrated that the segments constituting a chain with fixed ends are not isotropically oriented, but tend to be oriented along the end-to-end vector. This result implies that, if cross-links and trapped entanglements are fixed on the time scale of NMR observation, motions of elastic chain segments are not isotropic. Thus, transverse dephasing data associated with elastic chains may not conform to the exponential shape observed for unattached chains and pendant chains.

In his derivation, Cohen-Addad[31] determined the probability distribution function, $P(\vec{a}|\vec{r})$, of orientations of any segment, $\vec{a}$, in a chain with fixed end-to-end vector, $\vec{r}$:

$$P(\vec{a}|\vec{r}) = \frac{1}{4\pi}\exp\left(\frac{\vec{a}\cdot\vec{r}}{\sigma^2}\right) \tag{19}$$

where σ represents the contour length of the chain. This probability distribution function was used to average the magnetic interaction, $\omega(t)$, over all orientations compatible with $\vec{r}$ to give the transverse dephasing function, $e(t)$, for a segment in a single chain with fixed end-to-end vector:

$$e(t) = \cos[\langle\omega(\vec{a}(t))\rangle t] \tag{20}$$

The quantity in brackets represents the partial average of the magnetic interaction over all orientations compatible with a given, fixed end-to-end vector. The transverse dephasing function, $E(t)$, for an entire sample was then obtained by averaging the transverse dephasing curve, $e(t)$, expected for end-to-end vector, $\vec{r}$, over a Gaussian distribution, $P(\vec{r})$, of end-to-end vectors:

$$E(t) = \int \mathrm{d}\vec{r}\ P(\vec{r})e(t) \tag{21}$$

As shown by Cohen-Addad and Dupeyre,[32] this function is expressed most conveniently by defining the second moment, M_2, of $e(t)$:

$$M_2 = -\int \left(\frac{\mathrm{d}^2 e(t)}{\mathrm{d}t^2}\right)_{t=0} P(\vec{r})\ \mathrm{d}\vec{r} = \int \langle \omega(\vec{a}(t)) \rangle^2 P(\vec{r})\ \mathrm{d}\vec{r} \tag{22}$$

Using this definition, $E(t)$ may then be expressed as

$$E(t) = \left[\frac{1 + 3\phi^2 + [(1 + 3\phi^2)^2 + 4\phi^6]^{1/2}}{2[(1 + 3\phi^2)^2 + 4\phi^6]}\right]^{1/2} \tag{23}$$

where $\phi = t(M_2/3)^{1/2}$. Using (19) to average the magnetic interaction, ω, it can be shown that the second moment is inversely proportional to the square of the number of statistical segments along the contour of a chain with fixed end-to-end vector.[32] Thus, we expect that transverse dephasing functions associated with deuterons in elastic chains will be characterized by a single parameter, which is inversely proportional to the square of the number-average molecular weight of an effective elastic chain. Here, an effective elastic chain consists of all of the material which extends between constraints that are fixed on the time scale of NMR observation. Besides chemical cross-links, trapped topological entanglements may also act as such constraints.

The transverse dephasing for an elastomer is obtained by combining the expressions for transverse dephasing for pendant and elastic chains:

$$M(t) = f_{\mathrm{el}}E(t,t_{\mathrm{el}}) + (1 - f_{\mathrm{el}})P(t,t_{\mathrm{pen}}) \tag{24}$$

This expression has three parameters: the weight fraction of elastic chains and the characteristic dephasing times, t_{pen} and t_{el}, for pendant and elastic chains, respectively. We have defined t_{el} to be the inverse square root of the second moment, M_2, given in (22). Each of these adjustable parameters may be related to the structure of the elastomer. Based on the model proposed by Cohen-Addad and Dupeyre,[32] t_{el} is expected to be directly proportional to the number-average molecular weight of elastic chains in the network. According to the BPP formalism,[27] t_{pen} is expected to increase as f_{el} decreases and M_c increases, enabling increased segment mobility.

Solid curves in Figure 3 represent least squares fits to the three-parameter model given in eq 24; parameters obtained from the fits are listed in Table 4. The fractions of elastic chains obtained from NMR measurements decrease monotonically as those obtained from the Macosko−Miller model, which are listed in Table 2, but the fraction of elastic chains obtained as a parameter of the ^{2}H-NMR model is consistently higher than that predicted by the statistical model. We postulate that this difference is because portions of pendant chains that are entangled may not have time to isotropically reorient on the NMR time scale and thus contribute to the elastic component of the spectrum. Figure 5 suggests that elastic chain time constants are directly proportional to elastic chain molecular weights obtained from swelling measurements, as predicted by the Cohen-Addad model.[31] The time constants for pendant chain dephasing increase with increasing M_c and decreasing f_{el}, as expected. The correlation between the characteristic dephasing time for elastic chains and

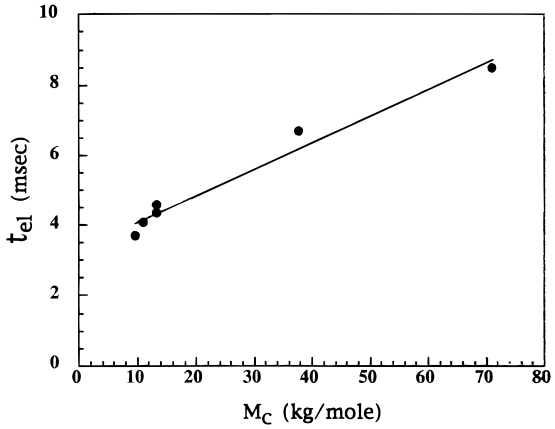

Figure 5. Molecular weight dependence of elastic chain dephasing time constant, t_{el}. Time constants are calculated as inverse square roots of second moments of elastic chain spectra. Number-average molecular weights, M_c, of elastic chains have been obtained from equilibrium swelling measurements. The solid line represents the best fit to a straight line.

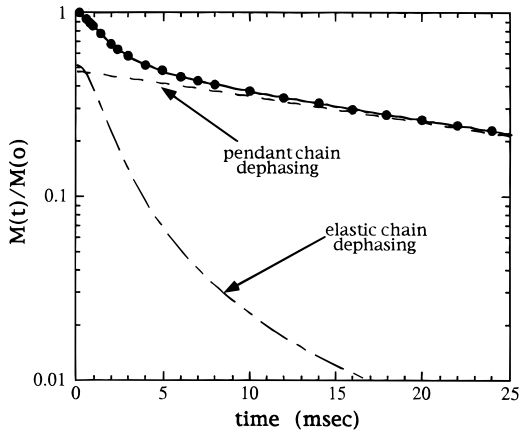

Figure 6. Simulated ^{2}H-NMR dephasing curves for PDMS-(d) network A-4. The solid line gives the total fit using eq 24; the curve with alternating long and short dashes gives the elastic chain contribution to the transverse dephasing; the dashed line gives the pendant chain contribution.

the elastic chain molecular weight obtained from swelling measurements suggests that both entanglements and cross-links limit the motion which averages the quadrupolar interaction in accord with the observation of inhomogeneous line broadening for entangled linear polymers.

Because elastic chain segments are less mobile than pendant chain segments, deuterons associated with elastic chains dephase more rapidly than those associated with pendant chains. This dephasing rate difference is illustrated in Figure 6, which gives the individual components of the dephasing curve simulated using eq 24 with parameters for PDMS(d) network A-4. The solid curve represents the total dephasing curve, the dashed line gives the pendant chain component, and the line with alternating long and short dashes gives the elastic chain component. Based on this difference in dephasing rates, we have developed an empirical method to obtain direct, experimental observations of pendant or elastic chain ^{2}H-NMR data in a single elastomer network. Independent observations of pendant and elastic chains are obtained by observing two spectra using the $(90°)_x-\tau-(180°)_y-\tau$ pulse sequence. The first (Figure 7a) is obtained using a τ delay that is as short as possible ($\tau = 0.1$ ms). Because this spectrum is observed after essentially no dephasing has yet taken

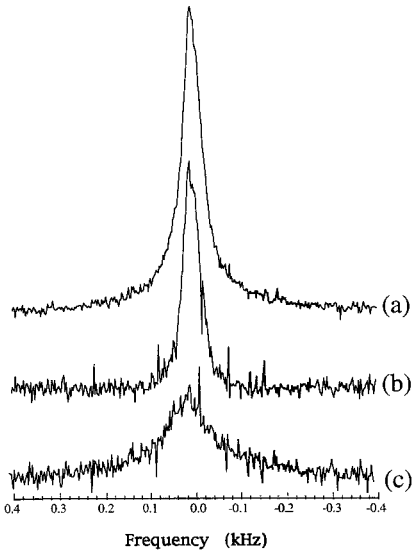

Figure 7. ^{2}H-NMR spectra of PDMS(d) network A-4 measured with $(90°)_x-\tau-(180°)_y-\tau$ pulse sequence: (a) spectrum obtained at $\tau = 0.1$ ms (total area has been normalized); (b) spectrum obtained at $\tau = 10$ ms (area has been normalized and scaled by fraction of pendant chains obtained from ^{2}H-NMR results); (c) spectrum obtained by subtracting (b) from (a).

place, we propose that it is made up of both the pendant chain and elastic chain contributions to magnetization. The second spectrum (Figure 7b) is obtained using a long delay ($\tau = 10$ ms), and it represents the magnetization following quadrupolar dephasing during a time period of 20 ms. According to our model, the elastic chain contribution to this long-τ spectrum is negligible, because the elastic chain magnetization has dephased to an intensity more than an order of magnitude smaller than that of the pendant chains. Thus, this second spectrum is essentially an observation of deuterons in pendant chains. The elastic chain spectrum (Figure 7c) is obtained by subtracting the pendant chain spectrum, scaled by the fraction of pendant chains obtained from NMR measurement, from the total spectrum.

V. Summary

Deuterated elastomers with systematically varied structures have been produced by end-linking known fractions of monofunctional and difunctional PDMS(d) chains with a tetrafunctional cross-linking agent. The networks have been characterized by analyzing their elasticity and swelling measurements in terms of well-established models. ^{2}H-NMR observations of these well-characterized PDMS networks indicate increased motional averaging of the orientation-dependent quadrupolar interaction with decreasing fractions and increasing number-average molecular weights of elastic chains. Transverse ^{2}H-NMR dephasing data obtained for the networks are well represented by a sum of two components, one of which was attributed to pendant chains, and the other to elastic chains. This simple model has three adjustable parameters: the weight fraction of elastic chains and a characteristic dephasing time for each component. Best fits of the model to the ^{2}H-NMR data obtained for randomly-deuterated elastomers give parameter values which are correlated with structural parameters inferred from statistical and swelling measurements. The success of the two-component model in representing elastomer data suggests that ^{2}H-NMR differentiates between pendant and elastic chains on the basis of their mobility differences. Based on this sensitivity, an empirical method has been developed which decouples pendant and elastic chain contributions to the ^{2}H-NMR spectrum of a deuterated network.

Acknowledgment. We are grateful to the National Science Foundation, which provided support for this work in the form of a Graduate Fellowship for K.M. The authors thank Shawn Malone for many helpful discussions concerning the synthesis procedures used herein.

References and Notes

(1) Abragam, A. *The Principles of Nuclear Magnetism*; Clarendon Press: Oxford, 1961.
(2) Jelinski, L. *Annu. Rev. Mater. Sci.* **1985**, *15*, 359.
(3) Spiess, H. W. In *Adv. Polym. Sci.* **1985**, *66*, 23.
(4) Pake, G. E. *J. Chem. Phys.* **1948**, *16*, 327.
(5) Deloche, B.; Beltzung, M.; Herz, J. *J. Phys. (Paris), Lett.* **1982**, *43*, 763.
(6) Gronski, W.; Stadler, R.; Jacobi, M. *Macromolecules* **1984**, *17*, 741.
(7) Sotta, P.; Deloche, B.; Herz, J.; Lapp, A.; Durand, D.; Rabadeux, J. *Macromolecules* **1987**, *20*, 2769.
(8) Sotta, P.; Deloche, B. *Macromolecules* **1990**, *23*, 1999.
(9) Kornfield, J.; Chung, G.; Smith, S. *Macromolecules* **1992**, *25*, 4442.
(10) Simon, G.; Baumann, K.; Gronski, W. *Macromolecules* **1992**, *25*, 3624.
(11) Patel, S.; Malone, S.; Cohen, C.; Gillmor, J.; Colby, R. *Macromolecules* **1992**, *25*, 5241.
(12) Malone, S.; Vosburgh, C.; Cohen, C. *Polymer* **1993**, *34*, 5149.
(13) Venkataraman, S. K.; Coyne, L.; Chambon, F.; Gottlieb, M.; Winter, H. H. *Polym. Prepr. (Am. Chem. Soc., Div. Polym. Chem.)* **1988**, *29*, 571.
(14) Lee, C. L.; Frye, C. L.; Johannson, O. K. *Polym. Prepr. (Am. Chem. Soc., Div. Polym. Chem.)* **1969**, *10*, 1361.
(15) Lee, C. L.; Johannson, O. K. *J. Polym. Sci., Polym. Chem. Ed.* **1976**, *14*, 729.
(16) Lee, C. L.; Marko, O. W.; Johannson, O. K. *J. Polym. Sci., Polym. Chem. Ed.* **1976**, *14*, 743.
(17) Lapp, A.; Herz, J.; Strazielle, C. *Makromol. Chem.* **1985**, *186*, 1919.
(18) Beltzung, M.; Picot, C.; Rempp, P.; Herz, J. *Macromolecules* **1982**, *15*, 1594.
(19) Weiss, P.; Herz, J.; Rempp, P. *Makromol. Chem.* **1970**, *135*, 249.
(20) Macosko, C. W.; Miller, D. R. *Macromolecules* **1976**, *9*, 199.
(21) Miller, D. R.; Macosko, C. W. *Macromolecules* **1976**, *9*, 206.
(22) Miller, D. R.; Valles, E. M.; Macosko, C. W. *Polym. Eng. Sci.* **1979**, *19*, 272.
(23) Flory, P. J.; Rehner, J. *J. Chem. Phys.* **1943**, *11*, 521.
(24) Flory, P. J. *Principles of Polymer Chemistry*; Cornell University Press: Ithaca, NY, 1953.
(25) James, H. M.; Guth, E. J. *J. Chem. Phys.* **1947**, *15*, 669.
(26) Fedotov, V.; Chernov, V.; Khazanovich, T. *Vysokomol. Soedin.* **1978**, *A20*, 919.
(27) Poon, C.; Samulski, E.; Nakatani, A. *Makromol. Chem., Makromol. Symp.* **1990**, *40*, 109.
(28) Poon, C.; Samulski, E. *J. Non-Cryst. Solids* **1991**, *131*, 509.
(29) Bloembergen, N.; Purcell, E.; Pound, R. *Phys. Rev.* **1948**, *73*, 679.
(30) See, for example: Goldman, M. *Quantum Description of High-Resolution NMR in Liquids*; Clarendon Press: Oxford, 1988; Chapter 9.
(31) Cohen-Addad, J. P. *J. Chem. Phys.* **1976**, *64*, 8, 3438.
(32) Cohen-Addad, J. P.; Dupeyre, R. *Polymer* **1983**, *24*, 400.

MA9600320